RSC Advances

PAPER

View Article Online
View Journal | View Issue

Cite this: *RSC Adv.*, 2020, **10**, 29603

Transistor properties of salen-type metal complexes†

Kyohei Koyama, Kodai Iijima, Dongho Yoo ‡ and Takehiko Mori *

Received 21st June 2020
Accepted 3rd August 2020

DOI: 10.1039/d0ra05449f

rsc.li/rsc-advances

Schiff base complexes derived from salicylaldehyde and ethylene-, propylene-, and *trans*-1,2-cyclohexanediamines exhibit p-channel transistor properties. The Cu complexes are open-shell compounds, but the oxidation and the hole transport occur at the highest occupied molecular orbital, where the singly occupied molecular orbital (SOMO) does not participate in conduction. Although Ni complexes tend to show larger mobilities than Cu complexes owing to the molecular planarity, the presence of SOMO is not harmful to the transistor properties.

Introduction

Owing to the potential application to plastic electronics, a great deal of attention has been paid to organic semiconductors used in organic light-emitting diodes, transistors, and photovoltaics. Among organic semiconductors, metal complexes are promising materials but not sufficiently explored.[1] Square planar dithiolene complexes coordinated by four sulfur atoms ($M–S_4$) are strong electron acceptors with the lowest unoccupied molecular orbital (LUMO) level located around −4.2 eV, which show air-stable n-channel transistor properties.[2] Metal complexes coordinated by four nitrogen atoms ($M–N_4$) are exemplified by phthalocyanine,[3] which is a well known p-channel material. Several other $M–N_4$ systems show p-channel transistor properties.[4] A metal complex derived from 1,2-phenylenediamine is a strong electron donor,[5,6] whose highest occupied molecular orbital (HOMO) level is located at as high as −4.44 eV. However, owing to the small energy gaps, the phenylenediamine complexes exhibit ambipolar properties on an inert interface.[6,7] These results demonstrate that metal complexes realize very strong electron acceptor and donor abilities which are never attainable by ordinary organic materials, and at the same time very small energy gaps. Recently, infinite-sheet complexes of $M–S_4$ and $M–N_4$ are attracting attention as analogues of graphene; these complexes exhibit high electrical conductivity,[8] and even superconductivity.[9]

Inspired by these findings, we have investigated $M–N_2O_2$ complexes with more ordinary redox properties.[10] Schiff base complexes derived from salicylaldehyde and ethylene diamine are known as salen complexes (Scheme 1), which are moderate electron donors with the HOMO levels located around −5.3 eV. Electron and hole mobilities of 10^{-5} cm^2 V^{-1} s^{-1} have been reported in the time-of-flight measurement of an alkylthiophene-substituted salen complex.[11] High hole mobility of 1.5 cm^2 V^{-1} s^{-1} has been reported in a thiophene-based Schiff base of 1,2-phenylenediamine.[12] Hole mobility in the 10^{-7} cm^2 V^{-1} s^{-1} order has been also reported in a Schiff base with tetrathiafulvalene moieties.[13] In $M–N_2S_2$ complexes including thiosalen, we have recently found ambipolar transistor properties associated with energy gaps as small as 0.5–0.6 eV.[14] However, transistor properties are not investigated in the most fundamental salen complexes. In particular, all these Ni complexes are closed shell compounds, but open-shell Cu compounds have not been examined as transistors.

In the present work, we have investigated transistor properties of ethylenediamine (salen),[15–21] propylenediamine (salpn),[22] and *trans*-1,2-cyclohexanediamine (salcyh) complexes (Scheme 1).[23–26] Changing metal atoms, we can compare transistor properties of open- and closed-shell materials. A copolymer of salpn complex

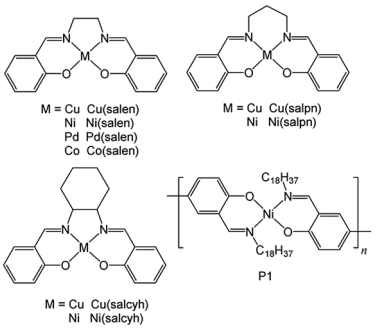

Scheme 1 Structures of salen-type metal complexes.

Department of Materials Science and Engineering, Tokyo Institute of Technology, Ookayama 2-12-1, Meguro-ku, 152-8552, Japan. E-mail: mori.t.ae@m.titech.ac.jp

† Electronic supplementary information (ESI) available: Additional information for preparative details, dimer energy levels, devices fabrication, AFM images, and transistor characteristics. See DOI: 10.1039/d0ra05449f

‡ Present address: Department of Chemical Engineering and Center for Advanced Soft Electronics, Pohang University of Science and Technology, 77 Cheongam-Ro, Nam-gu, Pohang 37673, Korea.

and thiophene has been reported to show conductivity of 83 mS cm^{-1}.[27] We have also examined conducting properties of a homopolymer containing Schiff base (**P1**).

Results and discussion

Electronic properties

The salen, salpn and salcyh complexes were prepared according to literature.[15–26,28] Since these complexes do not decompose up to high temperatures,[18,21] the materials were purified by sublimation, and the thin films were formed by vacuum evaporation.

The monomer ligand, 4,4′-dihydroxy-1,1′-biphenyl-3,3′-dicarboaldehyde, was prepared from 4,4′-dihydroxy-1,1′-biphenyl,[29] which was successively reacted with octadecyl amine and metal to afford the metal polymer (**P1**).

Cyclic voltammograms of these complexes show oxidation waves around 0.3–0.6 V (Fig. 1(a) and (b)). These complexes are moderate electron donors whose HOMO levels are located around −5.2 to −5.6 eV (Table 1).[11,26] The Cu and Co complexes are open shell materials,[19,23] but the observed oxidation waves seem to come from the HOMO (Fig. 2). The calculated singly occupied molecular orbital (SOMO) levels are located much above the HOMO (Fig. 2). Since these complexes are strongly dimerized in the crystals, we have carried out the calculations based on the dimers. The SOMO levels split to ±0.3 eV (Fig. S2†), but the resulting occupied levels (−3.8 to −4.2 eV) are still far from the observed E_{HOMO} in Table 1. The Cu complexes show slightly large oxidation potentials and deep HOMO levels in comparison with other complexes (Table 1). This is in complete agreement with the calculated HOMO levels (Fig. 2).

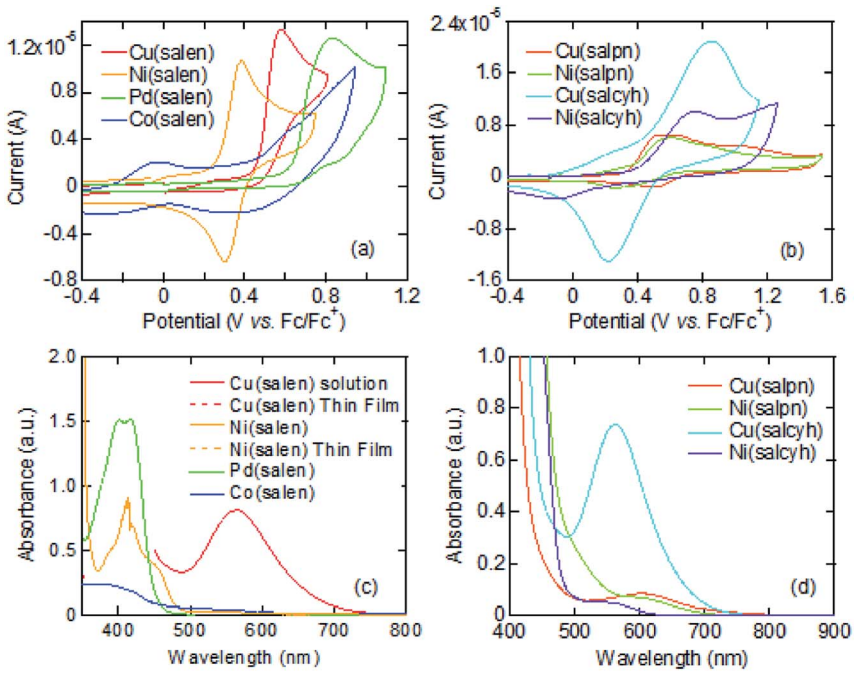

Fig. 1 (a and b) Cyclic voltammograms, and (c and d) absorption spectra.

Table 1 Oxidation potentials, energy levels, and optical gaps

Complex	$E_1^{1/2}$ (V)	E_{HOMO}[a] (eV)	λ_{edge}[b] (nm)	Optical gap[b] (eV)	E_{LUMO}[c] (eV)
Cu(salen)	0.48	−5.28 (−5.29)	438 (676)	2.83 (1.83)	−2.45 (−3.45)
Ni(salen)	0.34	−5.14 (−5.06)	496	2.50	−2.64
Pd(salen)	0.64	−5.36 (−5.17)	474	2.62	−2.73
Co(salen)	0.47	−5.27 (−5.13)	470	2.64	−2.63
Cu(salpn)	0.53	−5.33 (−5.18)	495 (824)	2.50 (1.50)	−2.83 (−3.78)
Ni(salpn)	0.44	−5.24 (−4.97)	510	2.40	−2.84
Cu(salcyh)	0.53	−5.33 (−5.43)	480 (737)	2.58 (1.68)	−2.75 (−3.57)
Ni(salcyh)	0.23	−5.03 (−4.95)	490	2.53	−2.53
P1	0.57	−5.13	482	2.57	−2.56

[a] The HOMO levels were estimated from the first oxidation potentials by assuming the reference energy level of ferrocene/ferrocenium to be 4.8 eV from the vacuum level.[30] The values in the parentheses were calculated by using the ADF software with the B3LYP* functional and TZP basis set.[31] [b] The values in the parentheses were from the dd transitions. [c] The LUMO levels were obtained from the HOMO levels and the optical gaps. The values in the parentheses were related to the SOMO levels.

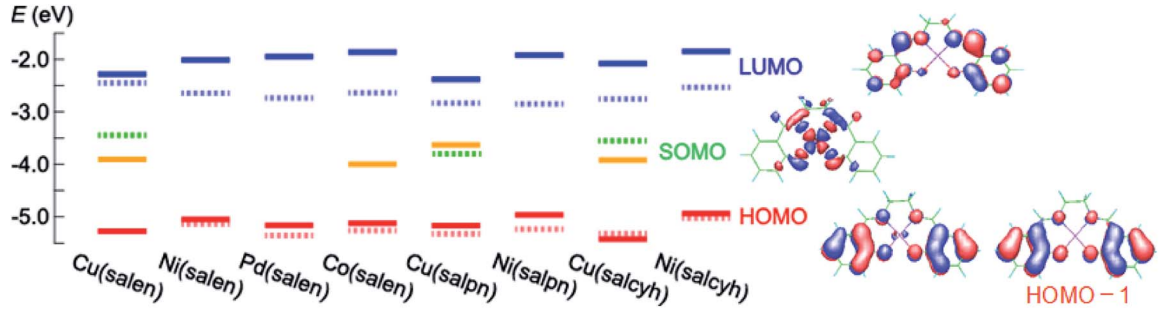

Fig. 2 Calculated (solid) and experimentally determined (dashed) energy levels as well as the molecular orbitals.

From these observations, the oxidation waves are attributed to the HOMO levels. Co(salen) exhibits another redox wave around 0 V (Fig. 1(a)), potentially related to the partially occupied HOMO level.[32]

The absorption edges around 490 nm come from the ππ* transitions in the Ni and Pd complexes (Fig. 1(c)), indicating the HOMO–LUMO gaps of 2.5 eV (Table 1).[16] This leads to the LUMO levels around −2.9 eV, which do not conflict with the calculated LUMO levels around −2.0 eV (Fig. 2). In addition, reduction waves are not observed, and electron conduction is unlikely.[30] In analogy with the M–N_2S_2 complexes,[14] this is partly because the two ligands are not conjugated.

The Cu complexes show an enhanced dd transition around 590 nm (Fig. 1(c) and (d)),[26] but this is much reduced in the thin films probably due to the dimerization. This transition suggests the presence of additional levels around −3.5 to −3.7 eV coming from the d-like SOMO levels. These orbitals are σ-like for the ligands (Fig. 2), and the oxidation occurs on the HOMO rather than the SOMO. It is expected from the HOMO levels that these complexes show hole conduction.[30]

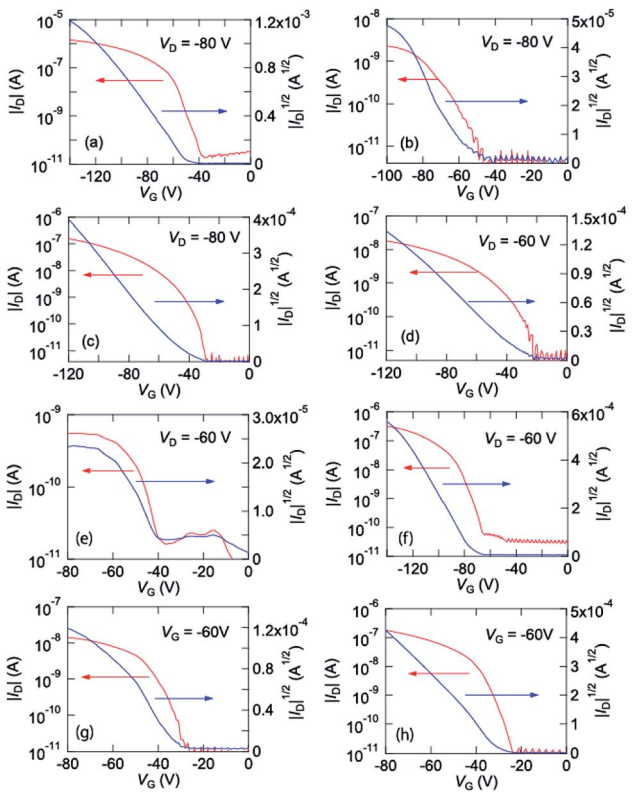

Fig. 3 Transfer characteristics of (a) Cu(salen), (b) Ni(salen), (c) Pd(salen), (d) Co(salen), (e) Cu(salpn), (f) Ni(salpn), (g) Cu(salcyh), and (h) Ni(salcyh).

Transistor properties

These complexes were vacuum evaporated on a SiO_2/Si substrate, and bottom-gate top-contact transistors were fabricated. These complexes show p-channel transistor properties as depicted in Fig. 3. From these characteristics, the transistor parameters are extracted as listed in Table 2. Cu(salen) shows maximum mobility of 4.3×10^{-3} cm^2 V^{-1} s^{-1}, but the Ni, Pd, and Co analogues show by more than one order lower mobilities.

Ni(salpn) and Ni(salcyn) exhibit comparable mobilities to Cu(salen), whereas Cu(salpn) and Cu(salcyn) show lower mobilities. In these two series, the closed-shell Ni complexes show higher mobilities than the open-shell Cu complexes.

Transfer integrals

Dimerized crystal structures have been reported in Cu(salen), Ni(salen), and Pd(salen) (Fig. 4),[33–36] where each dimer is arranged in an alternately tilted manner. Cu(salpn) and Ni(salpn) make loosely packed stacking structures.[22,37] Cu(salcyh) and Ni(salcyh) also have dimerized structures.[25,38]

In order to interpret the observed significant difference of the transistor performance, transfer integrals of the HOMO are investigated.[39,40] As shown in Fig. 4 and Table 3, the salen complexes form strongly dimerized herringbone structures, but the structures are not isostructural. Cu(salen) has a dihedral angle of ~140° (Fig. 4(a)), and the unit cell is elongated along the "stacking" (*c*) axis.[23] Parallel dimers are aligned along the horizontal (*b*) axis. Ni(salen) has a similar dihedral angle of ~140° (Fig. 2(b)), but the cell is elongated along the transverse (*a*) axis.[34] Parallel dimers are aligned along the vertical (*b*) axis. Pd(salen) (Fig. 4(c)) is similar to Ni(salen),[35] though the latter has a double layer structure along the *c* axis.

The intradimer transfer t_1 is as large as 200 meV (Table 3), and the other interdimer transfers are nearly by one order of magnitude smaller than t_1. $2t_1$ affords the splitting of the two energy bands, and t_2–t_4 give the bandwidth. In Cu(salen), t_4 makes a two-dimensional network (Fig. 4(a)), while t_2–t_4 are one

Table 2 Transistor characteristics of the thin-film transistors

Complex	μ_{max} ($cm^2\ V^{-1}\ s^{-1}$)	μ_{ave} ($cm^2\ V^{-1}\ s^{-1}$)	V_{th} (V)	On/off ratio
Cu(salen)	4.3×10^{-3}	2.5×10^{-3}	−45	10^5
Ni(salen)	6.1×10^{-5}	4.4×10^{-5}	−44	10^5
Pd(salen)	8.6×10^{-4}	5.4×10^{-4}	−60	10^5
Co(salen)	6.0×10^{-5}	4.3×10^{-5}	−32	10^5
Cu(salpn)	5.1×10^{-5}	2.9×10^{-5}	−37	10^3
Ni(salpn)	1.7×10^{-3}	1.0×10^{-3}	−83	10^5
Cu(salcyh)	2.6×10^{-4}	1.3×10^{-4}	−36	10^3
Ni(salcyh)	2.0×10^{-3}	1.4×10^{-3}	−28	10^4

half in Ni(salen) and Pd(salen). This may be related to the comparatively large mobility of Cu(salen). Co(salen) has only a highly one-dimensional interaction. Although not strictly isostructural, Ni(salen), Pd(salen), and Co(salen) have very similar molecular packing, and the two-dimensional network of Cu(salen) seems to be more advantageous to the charge transport.

The salpn complexes have uniform stacking structures with $t_1 \sim 100$ meV (Fig. 4(d) and (e)).[36] Although the molecular planarity is not very good, the interplanar distance is short (3.45 and 3.36 Å) and the adjacent molecule is located exactly on the top of another molecule. Therefore, the transfer is smaller than t_1 in the salen complexes (Table 3). Strong dimerization is not inherent in the present metal complexes, and the uniform chain does not seem to be too disadvantageous to the conduction.

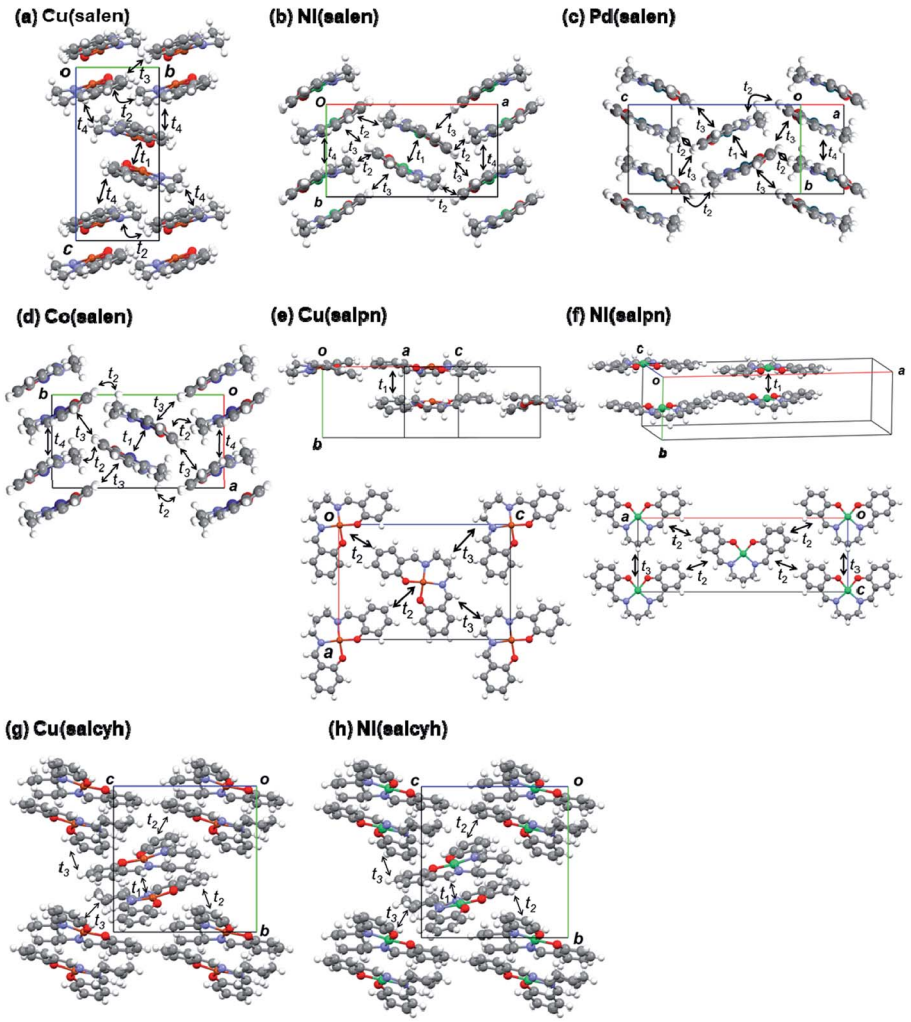

Fig. 4 Crystal structures and transfer integrals of (a) Cu(salen),[33] (b) Ni(salen),[34] (c) Pd(salen),[35] (d) Co(salen),[36] (e) Cu(salpn),[22,37] (f) Ni(salpn),[37] (g) Cu(salcyh),[25] and (h) Ni(salcyh).[38]

Table 3 Transfer integrals (meV) of the HOMO and sum of angles around the metal atom in the salen-type complexes

Complex	t_1	t_2	t_3	t_4	Angle (°)
Cu(salen)	237	−9	1	40	358.7
Ni(salen)	191	−9	15	21	358.6
Pd(salen)	212	−10	−22	−19	360.0
Co(salen)	−34	3	−27	−87	360.0
Cu(salpn)	−94	−6	−6		365.8
Ni(salpn)	−110	3	−9		359.4
Cu(salcyh)	189	−13	−4		361.7
Ni(salcyh)	102	−10	−25		360.1

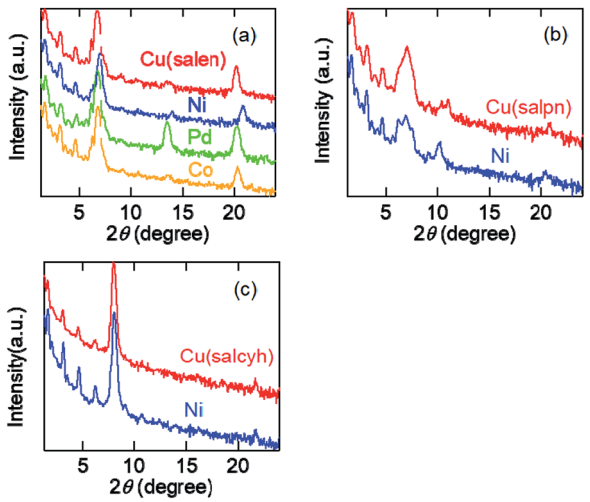

Fig. 5 (a) XRD patterns of evaporated films of the salen complexes. (b) XRD patterns of evaporated films of the salpn complexes. (c) XRD patterns of evaporated films of the salcyh complexes.

The salcyh complexes have strongly dimerized structures (Fig. 4(g) and (h)).[25,38] Nonetheless, Ni(salcyh) has larger inter-dimer interaction t_3 than Cu(salcyh), and this may be the origin of the difference of the mobility.

In order to investigate planarity of the complexes, sums of four bond angles around the metal atoms are compared in Table 3.[22,33–38] When the complex is planar, the angle is 360°. The deviation is particularly large in Cu(salpn),[22] related to the reduced transistor performance in comparison with Ni(salpn). Cu(salcyh) shows larger non-planarity than Ni(salcyh) as well. By contrast, non-planarity is not serious in Cu(salen) with a shorter alkyl diamine. The transistor performance seems to be closely related to the molecular planarity.

Table 4 XRD 2θ and d values

Complex	2θ (°)	d (Å)	Complex	2θ (°)	d (Å)
Cu(salen)	6.696	13.20	Cu(salpn)	6.979	12.67
Ni(salen)	6.956	12.71	Ni(salpn)	6.878	12.85
Pd(salen)	6.723	13.15	Cu(salcyh)	8.020	11.02
Co(salen)	6.761	13.07	Ni(salcyh)	8.062	10.97

Thin-film properties

Evaporated films of the salen complexes show sharp X-ray diffraction (XRD) peaks together with the higher-order peaks (Fig. 5(a)). The d-values are about 13 Å (Table 4), which are in good agreement with half of the crystallographic a (Cu) and c (Ni, Pd, and Co) axes.[33–36] We have observed several higher-order peaks. The molecules are standing perpendicular to the substrate keeping the crystallographic bc and ab planes parallel to the substrate.

The salpn complexes show XRD peaks at d = 12.7–12.8 Å (Fig. 3(b) and Table 4). These values correspond to the crystallographic b (Cu) and half of the a axes (Ni),[37] and the molecules are standing perpendicular to the substrate again. However, the comparatively broad peaks indicate that the crystallinity is not as good as the salen complexes.

Cu(salcyn) and Ni(salcyn) show sharp XRD peaks around 11.0 Å (Fig. 3(c) and Table 4). These values correspond to the crystallographic a axes. These molecules are standing perpendicular to the substrate, where the bc plane is parallel to the substrate.

Atomic force microscopy (AFM) images are shown in Fig. 6. These compounds form crystalline films; exceptions are Pd(salen) and Co(salen) (Fig. S4†). Cu(salen) shows large plate-like crystals, whereas other complexes exhibit needle-like crystals. The plate-like crystals are related to the two-dimensional electronic structure and the comparatively high mobility. Ni(salen) and Cu(salcyh) have rough surface, and probably this is associated with the relatively low mobility.

Polymer

Since an electrochemically prepared copolymer of VO(salen) and thiophene has been reported to show conductivity of 83 mS cm^{-1},[13] a homopolymer **P1** is chemically prepared. In

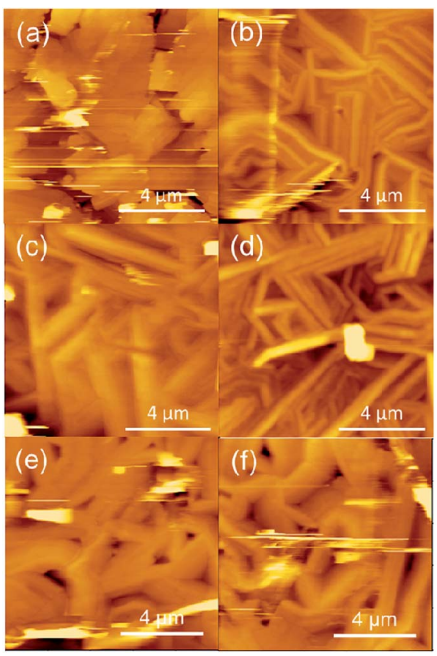

Fig. 6 Atomic force microscopy (AFM) images of (a) Cu(salen), (b) Ni(salen), (c) Cu(salpn), (d) Ni(salpn), (e) Cu(salcyh) and (f) Ni(salcyh).

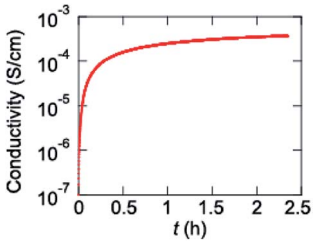

Fig. 7 Conductivity of P1 upon iodine doping.

contrast to the electrochemical polymers, the pristine polymer is entirely undoped. Since **P1** does not show transistor properties, **P1** is exposed to iodine vapor, where the conductivity increases from 1.0×10^{-7} to 3.7×10^{-4} S cm^{-1} (Fig. 7). The increase is saturated after about 30 min. When the sample is taken out from the iodine vapor, the conductivity decreases slightly, but is maintained around 0.8×10^{-4} S cm^{-1} for a long time (Fig. S6†). These results demonstrate efficient chemical hole doping is possible in **P1**.

Conclusions

We have demonstrated that salen-type metal complexes exhibit p-type transistor properties. Although Cu and Co complexes are open shell compounds,[19,23] the oxidation occurs at the same HOMO as the other metal complexes, and the hole transport is mediated by the HOMO. The SOMO does not participate in the oxidation and conduction due to the d-like character. Owing to the difference of the molecular packing and thin-film morphology, Cu(salen) shows larger mobility than other salen complexes, whereas the Ni salpn and salcyh complexes show larger mobilities than the Cu complexes. The latter is due to the molecular planarity of the Ni complexes, but the former example proves the presence of SOMO is not harmful to the transistor properties.

Although almost all organic semiconductors investigated so far are closed-shell materials,[4] copper phthalocyanine (CuPc) is an open-shell compound.[41] CuPc is an extensively investigated material,[3] but the SOMO is localized on the metal atom as well,[40] and the oxidation occurs at the HOMO.[42] Mobilities larger than 1 cm^2 V^{-1} s^{-1} have been reported in the single-crystal transistors,[3e,f] but the thin-film mobility is typically 0.02 cm^2 V^{-1} s^{-1},[3b] which is not largely different from the present materials. CuPc sometimes shows ambipolar transistor properties, but this has been attributed to the narrow-gap nature.[3f,7]

In mixed-stack charge-transfer complexes of tetracyanoquinodimethane (TCNQ),[43] the donor HOMO does not participate in the hole conduction, but hybridization of the donor next HOMO with the TCNQ LUMO leads to the electron-only transport. Similar to the present metal complexes, this is another example in which the most "frontier" orbital does not participate in the conduction, and a lower orbital mediates the charge transport owing to the larger intermolecular orbital overlap.

Conflicts of interest

There are no conflicts to declare.

Acknowledgements

This work was partly supported by the JSPS KAKENHI Grant Number 18H02044, and the Takahashi Industrial and Economic Research Foundation (08-003-022). The authors are grateful to Tokyo Institute of Technology Center for Advanced Materials Analysis for XRD measurement.

References

1 (*a*) T. Mori, *Chem. Lett.*, 2011, **40**, 428; (*b*) T. Mori, *J. Phys.: Condens. Matter*, 2008, **20**, 184010.
2 (*a*) E. C. P. Smits, T. D. Anthopoulos, S. Setayesh, E. van Veenendaal, R. Coehoorn, P. W. M. Blom, B. de Boer and D. M. de Leeuw, *Phys. Rev. B: Condens. Matter Mater. Phys.*, 2006, **73**, 205316; (*b*) T. D. Anthopoulus, S. Setayesh, E. Smits, M. Colle, E. Cantatore, B. Boer, P. W. M. Blom and D. M. de Leeuw, *Adv. Mater.*, 2006, **18**, 1900; (*c*) J. Cho, B. Domercq, S. C. Jones, J. Yu, X. Zhang, Z. An, M. Bishop, S. Barlow, S. R. Marder and B. Kippelen, *J. Mater. Chem.*, 2006, **17**, 2642; (*d*) T. Taguchi, H. Wada, T. Kambayashi, B. Noda, M. Goto, T. Mori, K. Ishikawa and H. Takezoe, *Chem. Phys. Lett.*, 2006, **421**, 395; (*e*) H. Wada, T. Taguchi, B. Noda, T. Kambayashi, T. Mori, K. Ishikawa and H. Takezoe, *Org. Electron.*, 2007, **8**, 759.
3 (*a*) L. Li, Q. Tang, H. Li and W. Hu, *J. Phys. Chem. B*, 2008, **112**, 10405; (*b*) Z. Bao, A. J. Lovinger and J. Lovinger, *Appl. Phys. Lett.*, 1996, **69**, 3066; (*c*) Z. Bao, A. J. Lovinger and J. Brown, *J. Am. Chem. Soc.*, 1998, **120**, 207; (*d*) R. Zeis, T. Siegrist and C. Kloc, *Appl. Phys. Lett.*, 2005, **86**, 022103; (*e*) L. Li, Q. Tang, H. Li, X. Yang, W. Hu, Y. Song, Z. Shuai, W. Xu, Y. Li and D. Zhu, *Adv. Mater.*, 2007, **19**, 2613; (*f*) R. W. I. de Boer, A. F. Stassen, M. F. Cracium, C. L. Mulder, A. Molinari, S. Rogge and A. F. Morpurgo, *Appl. Phys. Lett.*, 2005, **86**, 262109; (*g*) A. T. Vartanyan, *Zh. Fiz. Khim.*, 1948, **22**, 769.
4 (*a*) A. M. Whyte, Y. Shuku, G. S. nichol, M. M. Matsushita, K. Awaga and N. Robertson, *J. Mater. Chem.*, 2012, **22**, 17967; (*b*) M. Hunziker, B. Hilti and G. Rihs, *Helv. Chim. Acta*, 1981, **64**, 82.
5 (*a*) S. Noro, H. Chang, T. Takenobu, Y. Murayama, T. Kanbara, T. Aoyama, T. Sassa, T. Wada, D. Tanaka, S. Kitagawa, Y. Iwasa, T. Akutagawa and T. Nakamura, *J. Am. Chem. Soc.*, 2005, **127**, 10012; (*b*) S. Noro, T. Takenobu, Y. Iwasa, H. Chang, S. Kitagawa, T. Akutagawa and T. Nakamura, *Adv. Mater.*, 2008, **20**, 3399.
6 T. Kitamori, D. Yoo, K. Iijima, T. Kawamoto and T. Mori, *ACS Appl. Electron. Mater.*, 2019, **1**, 1633.
7 A. Opitz, M. Horlet, M. Kiwull, J. Wagner, M. Kraus and W. Brutting, *Org. Electron.*, 2012, **13**, 1614.
8 (*a*) T. Kambe, R. Sakamoto, T. Kusamoto, T. Pal, N. Fukui, K. Hoshiko, T. Shimojima, Z. Wang, T. Hirahara, K. Ishizaka, S. Hasegawa, F. Liu and H. Nishihara, *J. Am. Chem. Soc.*, 2014, **136**, 14357; (*b*) D. Sheberla, L. Sun, M. A. Blood-Forsythe, S. Er, C. R. Wade, C. K. Brozek, A. Aspuru-Guzik and M. Dinca, *J. Am. Chem. Soc.*, 2014, **136**, 8859.

9 X. Huang, L. Liu, L. Yu, G. Chen, W. Xu and D. Zhu, *Angew. Chem., Int. Ed.*, 2018, **57**, 146.
10 J. A. McClevery, *Prog. Inorg. Chem.*, 1968, **10**, 49.
11 L. Qu, D. Wang, C. Zhong, Y. Zou, J. Li, D. Zou and J. Qin, *Synth. Met.*, 2010, **160**, 2299.
12 A. K. Asatkar, S. P. Senanayak, A. Bedi, S. Panda, K. S. Narayan and S. S. Zade, *Chem. Commun.*, 2014, **50**, 7036.
13 (*a*) H. Nishikawa, A. Wachi, M. Chikamatsu and R. Azumi, *Mol. Cryst. Liq. Cryst.*, 2016, **641**, 81; (*b*) A. Wachi, Y. Kudo, A. Kanesaka, H. Nishikawa, T. Shiga, H. Oshio, M. Chikamatsu and R. Azumi, *Polyhedron*, 2017, **136**, 70.
14 Y. Kato, K. Iijima, D. Yoo, T. Kawamoto and T. Mori, *Chem. Lett.*, 2020, **49**, 870.
15 (*a*) R. H. Holm, *J. Am. Chem. Soc.*, 1960, **82**, 5632; (*b*) S. Di Bella, I. Fragala, I. Ledoux, M. A. Diaz-Garcia and T. J. Marks, *J. Am. Chem. Soc.*, 1997, **119**, 9550.
16 S. Zolezzi, A. Decinti and E. Spodine, *Polyhedron*, 1999, **18**, 897.
17 A. Nakahara, H. Yamamoto and H. Matsumoto, *Bull. Chem. Soc. Jpn.*, 1964, **37**, 1137.
18 Y. Nakao, N. Nonagase and A. Nakahara, *Bull. Chem. Soc. Jpn.*, 1969, **42**, 452.
19 G. D. Simpson, G. O. Calisle and W. E. Hatfield, *J. Inorg. Nucl. Chem.*, 1974, **36**, 2257.
20 K. J. Miller, J. H. Baag and M. M. Abu-Omar, *Inorg. Chem.*, 1999, **38**, 4510.
21 N. Kumari, R. Prajapati and L. Mishra, *Polyhedron*, 2008, **27**, 241.
22 (*a*) R.-G. Xiong, B.-L. Song, J.-L. Zuo and X.-Z. You, *Polyhedron*, 1996, **15**, 903; (*b*) L. C. Nathan, J. E. Koehne, J. M. Gilmore, K. A. Hannibal, W. E. Dewhirst and T. D. Mai, *Polyhedron*, 2003, **22**, 887.
23 R. S. Downing and F. L. Urbach, *J. Am. Chem. Soc.*, 1969, **91**, 5977.
24 R. S. Downing and F. L. Urbach, *J. Am. Chem. Soc.*, 1970, **92**, 5861.
25 K. Bernardo, S. Leppard, A. Robert, G. Commenges, F. Dahan and B. Meunier, *Inorg. Chem.*, 1996, **35**, 387.
26 I. C. Santos, M. Vilas-Boas, M. F. M. Piedade, C. Freire, M. T. Duarte and B. de Castro, *Polyhedron*, 2000, **19**, 655.
27 M. T. Nyuyen and B. J. Holliday, *Chem. Commun.*, 2015, **51**, 8610.
28 (*a*) R. H. Bailes and M. Calvin, *J. Am. Chem. Soc.*, 1947, **69**, 1886; (*b*) R. Warmuth and H. Elias, *Inorg. Chem.*, 1991, **30**, 5027.
29 Y. J. Lee, H. G. Heo and C. H. Oh, *Tetrahedron*, 2016, **72**, 6113.
30 M. L. Tang, A. D. Reicharrdt, P. Wei and Z. Bao, *J. Am. Chem. Soc.*, 2009, **131**, 5264.
31 *ADF2017.109, Scientific Computing & Modeling (SCM). Theoretical Chemistry*, Vrije Universiteit, Amsterdam, The Netherlands, https://www.scm.com.
32 A. Bottcher, T. Takeuchi, K. I. Hardcastle, T. J. Maeda, D. Cwikel, M. Kapon and Z. Dori, *Inorg. Chem.*, 1997, **36**, 2498.
33 (*a*) D. Hall and T. N. Waters, *J. Chem. Soc.*, 1960, 2644; (*b*) L. M. Shkol'nikova, E. M. Yumal', E. A. Shugam and V. A. Voblikova, *Zh. Strukt. Khim.*, 1970, **11**, 886; (*c*) A. G. Manfredotti and C. Guastini, *Acta Crystallogr., Sect. C: Cryst. Struct. Commun.*, 1983, **39**, 863; (*d*) E. F. DiMauro and M. C. Kozlowski, *Organometallics*, 2002, **21**, 1454; (*e*) M. Kondo, K. Nabari, T. Horiba, Y. Irie, M. K. Kabir, R. P. Sarker, E. Shimizu, Y. Shimizu and Y. Fuwa, *Inorg. Chem. Commun.*, 2003, **6**, 154.
34 M. A. Siegler and M. Lutz, *Cryst. Growth Des.*, 2009, **9**, 1194.
35 N. Kumari, R. Prajapati and L. Mishra, *Polyhedron*, 2008, **27**, 241.
36 W.-B. Yuan, H.-Y. Wang, J.-F. Du, S.-W. Chen and Q. Zhang, *Acta Crystallogr., Sect. E: Struct. Rep. Online*, 2006, **62**, m3504.
37 M. G. B. Drew, R. N. Prasad and R. P. Sharma, *Acta Crystallogr., Sect. C: Cryst. Struct. Commun.*, 1985, **41**, 1755.
38 A. Wojtczak, E. Szlyk, M. Jaskólski and E. Larsen, *Acta Chem. Scand.*, 1997, **51**, 274.
39 M. J. S. Dewar, E. G. Zoebisch, E. F. Healy and J. J. P. Stewart, *J. Am. Chem. Soc.*, 1985, **107**, 3902.
40 T. Mori, A. Kobayashi, Y. Sasaki, H. Kobayashi, G. Saito and H. Inokuchi, *Bull. Chem. Soc. Jpn.*, 1984, **57**, 627.
41 F. Evangelista, V. Carravetta, G. Stefani, B. Jansik, M. Alagia, S. Stranges and A. Ruocco, *J. Chem. Phys.*, 2007, **126**, 124709.
42 A. Wolberg and J. Manassen, *J. Am. Chem. Soc.*, 1970, **92**, 2982.
43 R. Sato, T. Kawamoto and T. Mori, *J. Mater. Chem. C*, 2019, **7**, 567.